

Combined Effects of Magnetic Field and Heat Source on Double-Diffusive Marangoni Convection in Fluid-Porous Structure



N. Manjunatha, Yellamma, and R. Sumithra

1 Introduction

In a variety of conditions, double-diffusive natural convection, or flows caused by buoyancy due to simultaneous temperature and concentration gradients, can occur. Some literature is available on the single and double component layer. Sumithra and Manjunatha [1] conducted an analytical study of magneto convection in a combined layer limited by adiabatic boundaries. Sankar et al. [2] and Jagadeesha et al. [3] examined the two-component convection using the Darcy model for porous enclosure in the presence of heat and solute source. Pushpa et al. [4] explored the thermosolutal convection. The influence of magnetic field on double-diffusive mixed convection in a rectangular inclined domain with an aspect ratio was investigated using a finite volume technique by Shivananda and Satheesh [5]. Shivakumara et al. [6] explored the effect of cross-diffusion on the beginning of convective instability. Sumithra and Arul Selvamary [7] discussed the single component convection for couple stress fluid in combined system for two boundary combinations. In the presence of magnetic field, heat generation or absorption, and chemical reaction, Xiaoli Qiang et al. [8] investigated unstable MHD double-diffusive convection flows between two infinite vertical parallel plates.

N. Manjunatha (✉)

Department of Mathematics, School of Applied Sciences, REVA University, Bengaluru, Karnataka, India

e-mail: manjunatha.n@reva.edu.in

Yellamma

School of Applied Sciences, REVA University, Bengaluru, Karnataka, India

R. Sumithra

Department of Mathematics, Nrupathunga University, Bengaluru, Karnataka, India

Peristaltically deformable and double-diffusive characteristics have been examined by Tanveer et al. [9].

Recently, the influence of a power law fluid and an angled magnetic field on a porous material in a staggered cavity is studied by Hussain et al. [10]. The influence of the Soret and Dufour factors is also considered. Meften [11] investigated two models of double-diffusive convection in a fluid layer where viscosity varies quadratically with temperature and nonlinear results are obtained using conditional energy analysis. Manjunatha et al. [12] and Manjunatha and Sumithra [13] studied the effects of three profiles and a heat source on convection in a combined structure in the presence of magnetic field. In the present study, the effect of magnetic field and heat source on onset convection is examined in detail for two types of boundary combinations.

2 Mathematical Formulation

Consider a double component, electrically conducting liquid saturated isotropic, sparsely packed porous layer of thickness d_p with an imposed magnetic field intensity H_0 underlying a triple component liquid layer of thickness d_f and with heat sources Φ_p and Φ_f , respectively. The porous layer's lower surface is hard, while the fluid layer's upper surface is free, with surface tension effects depending on temperature and concentration as shown in Fig. 1. A Cartesian coordinate system (x, y, z) is used with the origin at the interface between the porous and fluid layers, and the z -axis is vertically upward. Let ΔT and ΔC be the temperature and concentration difference between the lower and upper boundaries, $T = T_0$ the reference temperature, and $C = C_0$ the reference salinity. With the Boussinesq

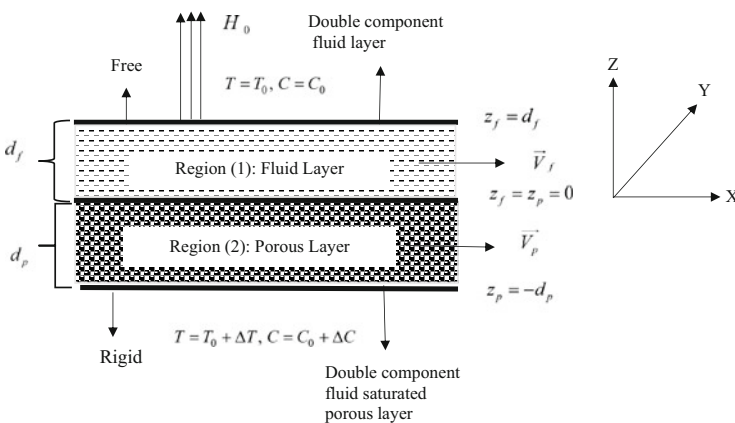


Fig. 1 Geometry of the problem

approximation, the basic equations for region 1 and region 2 (see Sumithra and Manjunatha [1] and Shivakumara et al. [14]).

Fluid layer: Region 1

$$\nabla_f \cdot \vec{V}_f = 0 \quad (1)$$

$$\nabla_f \cdot \vec{H} = 0 \quad (2)$$

$$\frac{\partial \vec{V}_f}{\partial t} + (\vec{V}_f \cdot \nabla_f) \vec{V}_f = -\frac{1}{\rho_0} \nabla_f P_f + \frac{\mu_f}{\rho_0} \nabla_f^2 \vec{V}_f + \frac{\gamma_f}{\rho_0} (\vec{H} \cdot \nabla_f) \vec{H} \quad (3)$$

$$\frac{\partial T_f}{\partial t} + (\vec{V}_f \cdot \nabla_f) T_f = \kappa_f \nabla_f^2 T_f + \Phi_f \quad (4)$$

$$\frac{\partial C_f}{\partial t} + (\vec{V}_f \cdot \nabla_f) C_f = \kappa_{cf} \nabla_f^2 C_f \quad (5)$$

$$\frac{\partial \vec{H}}{\partial t} = \nabla_f \times \vec{V}_f \times \vec{H} + \nu_f \nabla_f^2 \vec{H} \quad (6)$$

Porous layer: Region 2

$$\nabla_p \cdot \vec{V}_p = 0 \quad (7)$$

$$\nabla_p \cdot \vec{H} = 0 \quad (8)$$

$$\frac{1}{\varepsilon_p} \frac{\partial \vec{V}_p}{\partial t} + \frac{1}{\varepsilon_p^2} (\vec{V}_p \cdot \nabla_p) \vec{V}_p = -\frac{1}{\rho_0} \nabla_p P_p - \frac{\mu_p}{K \rho_0} \vec{V}_p + \frac{\gamma_p}{\rho_0} (\vec{H} \cdot \nabla_p) \vec{H} \quad (9)$$

$$M \frac{\partial T_p}{\partial t} + (\vec{V}_p \cdot \nabla_p) T_p = \kappa_p \nabla_p^2 T_p + \Phi_p \quad (10)$$

$$\phi_p \frac{\partial C_p}{\partial t} + (\vec{V}_p \cdot \nabla_p) C_p = \kappa_{cp} \nabla_p^2 C_p \quad (11)$$

$$\phi_p \frac{\partial \vec{H}}{\partial t} = \nabla_p \times \vec{V}_p \times \vec{H} + \nu_p \nabla_p^2 \vec{H} \quad (12)$$

where the fluid and porous regions are denoted by the subscripts f and p, respectively. \vec{V}_f is the velocity vector, ρ_0 is the fluid density, μ_f is the fluid viscosity, P_f is the total pressure, \vec{H} is the magnetic field, T_f is the temperature, ν_f is the magnetic viscosity, γ_f is the magnetic permeability, κ_{cf} is the solute diffusivity of the fluid, and C_f is the salinity field. For region 2, ϕ_p is the porosity, K is the permeability, M is the heat capacity ratio, κ_p is the thermal diffusivity, and ν_p is the effective magnetic viscosity.

The goal of this research is to see if a quiescent state can withstand tiny perturbations superimposed on the basic state; the solutions are as follows:

$$\vec{V}_f = 0, P_f = P_{fb}(z_f), T_f = T_{fb}(z_f), C_f = C_{fb}(z_f), \vec{H} = H_0(z_f) \quad (13)$$

$$\vec{V}_p = 0, P_p = P_{pb}(z_p), T_p = T_{pb}(z_p), C_p = C_{pb}(z_p), \vec{H} = H_0(z_p) \quad (14)$$

where

$$T_{fb}(z_f) = \frac{-\Phi_f z_f(z_f - d_f)}{2\kappa_f} + \frac{(T_u - T_0)z_f}{d_f} + T_0 \quad 0 \leq z_f \leq d_f$$

$$T_{pb}(z_p) = \frac{-\Phi_p z_p(z_p + d_p)}{2\kappa_p} + \frac{(T_0 - T_l)z_p}{d_p} + T_0 \quad -d_p \leq z_p \leq 0$$

$$C_{fb}(z_f) = C_0 - \frac{(C_0 - C_u)z_f}{d_f} \quad 0 \leq z_f \leq d_f$$

$$C_{pb}(z_p) = C_0 - \frac{(C_l - C_0)z_p}{d_p} \quad -d_p \leq z_p \leq 0$$

$$T_0 = \frac{\kappa_f d_p T_u + \kappa_p d_f T_l}{\kappa_f d_p + \kappa_p d_f} + \frac{d_f d_p (\Phi_p d_p + \Phi_f d_f)}{2(\kappa_f d_p + \kappa_p d_f)}, C_0 = \frac{\kappa_c d_p C_u + \kappa_{cp} d_f C_l}{\kappa_c d_p + \kappa_{cp} d_f}.$$

To investigate the stability of the basic state, regions 1 and 2 are subjected to infinite perturbations:

$$\vec{V}_f = \vec{V}'_f, P_f = P_{fb} + P'_f, T_f = T_{fb}(z_f) + \theta'_f, C_f = C_{fb}(z_f) + S'_f, \vec{H} = H_0(z_f) + \vec{H}' \quad (15)$$

$$\vec{V}_p = \vec{V}'_p, P_p = P_{pb} + P'_p, T_p = T_{pb}(z_p) + \theta'_p, C_p = C_{pb}(z_p) + S'_p, \vec{H} = H_0(z_p) + \vec{H}' \quad (16)$$

where $\vec{V}'_f, P'_f, \theta'_f, S'_f, \vec{H}'$ velocity, pressure, temperature, salinity, and magnetic field are respectively perturbed quantities for region 1 and the similar quantities in region 2 are $\vec{V}'_p, P'_p, \theta'_p, S'_p, \vec{H}'$. The variables are nondimensionalized for regions 1 and 2 using $d_f, \frac{d_f^2}{\kappa_f}, \frac{\kappa_f}{d_f}, T_0 - T_u, C_0 - C_u, H_0$, and $d_p, \frac{d_p^2}{\kappa_p}, \frac{\kappa_p}{d_p}, T_l - T_0, C_l - C_0, H_0$.

We arrive at the following stability equations in region 1 and region 2, respectively, using the conventional linear stability analysis approach and assuming that the concept of exchange of stability holds (see Sumithra and Manjunatha [1] and Shivakumara et al. [14]):

$$\left((D_f^2 - a_f^2)^2 - Q_f D_f^2 \right) W_f(z_f) = 0 \quad (17)$$

$$(D_f^2 - a_f^2)\theta_f(z_f) + \left(1 + R_{I_f}^*(2z_f - 1) \right) W_f(z_f) = 0 \quad (18)$$

$$\tau_f(D_f^2 - a_f^2)S_f(z_f) + W_f(z_f) = 0 \quad (19)$$

$$\left((D_p^2 - a_p^2) + Q_p \beta^2 D_p^2 \right) W_p(z_p) = 0 \tag{20}$$

$$(D_p^2 - a_p^2) \theta_p(z_p) + \left(1 + R_{Ip}^* (2z_p + 1) \right) W_p(z_p) = 0 \tag{21}$$

$$\tau_p (D_p^2 - a_p^2) S_p(z_p) + W_p(z_p) = 0 \tag{22}$$

In the above equations, $a_f, a_p, Q_f, Q_p, R_{If}^* = \frac{R_{if}}{2(T_0 - T_u)}, R_{Ip}^* = \frac{R_{ip}}{2(T_l - T_0)}, R_{if} = \frac{\Phi_f d_f^2}{\kappa_f}, R_{ip} = \frac{\Phi_p d_p^2}{\kappa_p}, \tau_f = \frac{\kappa_{cf}}{\kappa_f},$ and $\tau_p = \frac{\kappa_{cp}}{\kappa_p}$ are, namely, the horizontal wave numbers, the Chandrasekhar numbers, the modified internal Rayleigh numbers, the internal Rayleigh numbers, and the diffusivity ratios, $\beta = \sqrt{\frac{K}{d_p^2}}$ is the porous parameter, $W_f(z_f)$ and $W_p(z_p)$ are the vertical velocities, $\theta_f(z_f)$ and $\theta_p(z_p)$ are the temperatures, and $S_f(z_f)$ and $S_p(z_p)$ are the concentration distributions. Because the wave numbers for the combined layers must be the same, so that we have $\frac{a_f}{d_f} = \frac{a_p}{d_p}$ and hence $a_p = \hat{d} a_f$, here $\hat{d} = \frac{d_p}{d_f}$ is the depth ratio.

The boundary conditions are nondimensionalized after:

$$D_f^2 W_f(1) + (M_t \theta_f(1) + M_s S_f(1)) a_f^2 = 0 \tag{23}$$

The velocity conditions are

$$\begin{aligned} W_f(1) = 0, W_p(-1) = 0, D_p W_p(-1) = 0, \hat{T} W_f(0) = W_p(0), \\ \hat{T} \hat{d}^2 (D_f^2 + a_f^2) W_f(0) = \hat{\mu} (D_p^2 + a_p^2) W_p(0), \hat{T} \hat{d} D_f W_f(0) = D_p W_p(0), \\ \hat{T} \hat{d}^3 \beta^2 [(D_f^3 - 3a_f^2 D_f)] W_f(0) = [-D_p + \hat{\mu} \beta^2 (D_p^3 - 3a_p^2 D_p)] W_p(0) \end{aligned} \tag{24}$$

The conditions for adiabatic-adiabatic and adiabatic-isothermal, respectively, are

$$D_f \theta_f(1) = 0, \theta_f(0) = \hat{T} \theta_p(0), D_f \theta_f(0) = D_p \theta_p(0), D_p \theta_p(-1) = 0 \tag{25}$$

$$D_f \theta_f(1) = 0, \theta_f(0) = \hat{T} \theta_p(0), D_f \theta_f(0) = D_p \theta_p(0), \theta_p(-1) = 0 \tag{26}$$

The salinity conditions are

$$D_f S_f(1) = 0, S_f(0) = \hat{S} S_p(0), D_f S_f(0) = D_p S_p(0), D_p S_p(-1) = 0 \tag{27}$$

In the above equations, \hat{S} is the solute diffusivity ratio, \hat{T} is the thermal ratio, $\hat{\mu}$ is the viscosity ratio, $M_t = \frac{\partial \sigma_t}{\partial T_f} \frac{(T_u - T_0) d_f}{\mu_f \kappa_f}$ is the thermal Marangoni number (tMn), $M_s = \frac{\partial \sigma_t}{\partial C_f} \frac{(C_u - C_0) d_f}{\mu_f \kappa_f}$ is the solute Marangoni number (sMn), and σ_t is the surface tension.

3 Methodology

Introducing (24), the velocity profiles are obtained by solving (17) and (20) and appropriately written as follows:

$$W_f(z_f) = A_1 [\cosh \psi_f z_f + a_1 \sinh \psi_f z_f + a_2 \cosh \varphi_f z_f + a_3 \sinh \varphi_f z_f] \quad (28)$$

$$W_p(z_p) = A_1 [a_4 \cosh \delta_p z_p + a_5 \sinh \delta_p z_p] \quad (29)$$

where

$$\begin{aligned} \psi_f &= \frac{\sqrt{Q_f} + \sqrt{Q_f + 4a_f^2}}{2}, \varphi_f = \frac{\sqrt{Q_f} - \sqrt{Q_f + 4a_f^2}}{2}, \delta_p = \sqrt{\frac{a_p^2}{1 + Q_p \beta^2}}, a_1 = -\frac{a_3 \Delta_2}{\Delta_1}, \\ a_2 &= \frac{\Delta_5 \Delta_7 - \Delta_8 \Delta_4}{\Delta_3 \Delta_7 - \Delta_6 \Delta_4}, a_3 = \frac{\Delta_5 \Delta_6 - \Delta_8 \Delta_3}{\Delta_4 \Delta_6 - \Delta_7 \Delta_3}, a_4 = \hat{T}(1 + a_2), a_5 = \frac{1}{\delta_p} (\hat{T} \hat{d} a_1 \psi_f + a_3 \varphi_f) \\ \Delta_1 &= \hat{d}^2 \beta^2 (\psi_f^3 - 3a_f^2 \psi_f) + \psi_f, \Delta_2 = \hat{d}^2 \beta^2 (\varphi_f^3 - 3a_f^2 \varphi_f) + \varphi_f, \\ \Delta_3 &= \hat{T} \cosh \delta_p, \Delta_4 = -\frac{\hat{d} \hat{T} \sinh \delta_p}{\delta_p} (\varphi_f - \frac{\Delta_2 \psi_f}{\Delta_1}), \Delta_5 = -\Delta_3, \Delta_6 = \cosh \varphi_f, \\ \Delta_7 &= \sinh \varphi_f - (\frac{\Delta_2}{\Delta_1}) \sinh \psi_f, \Delta_8 = -\cosh \psi_f. \end{aligned}$$

Introducing (19) and (22), the salinity profiles are obtained using the condition (27), as follows:

$$S_f(z_f) = A_1 [c_{13} \cosh a_f z_f + c_{14} \sinh a_f z_f + \Sigma_{f1}(z_f)] \quad (30)$$

$$S_p(z_p) = A_1 [c_{15} \cosh a_p z_p + c_{16} \sinh a_p z_p + \Sigma_{p1}(z_p)] \quad (31)$$

where $\Sigma_{f1}(z_f) = \frac{-1}{\tau_f} \left[\frac{\cosh \psi_f z_f + a_1 \sinh \psi_f z_f}{\psi_f^2 - a_f^2} + \frac{a_2 \cosh \varphi_f z_f + a_3 \sinh \varphi_f z_f}{\varphi_f^2 - a_f^2} \right],$

$$\Sigma_{p1}(z_p) = \frac{-1}{\tau_p} \left[\frac{a_4 \cosh \delta_p z_p + a_5 \sinh \delta_p z_p}{\delta_p^2 - a_p^2} \right], c_{13} = \hat{S} c_{15} + \Delta_{100} + \Delta_{101},$$

$$c_{14} = \frac{1}{a_f} (c_{16} a_p + \Delta_{102} + \Delta_{103}), c_{15} = \frac{\Delta_{108} a_p \cosh a_p - \Delta_{107} \Delta_{105}}{a_p \sinh a_p \Delta_{107} + \Delta_{106} a_p \cosh a_p},$$

$$c_{16} = \frac{\Delta_{105} \Delta_{106} + a_p \sinh a_p \Delta_{108}}{a_p \sinh a_p \Delta_{107} + \Delta_{106} a_p \cosh a_p}, \Delta_{100} = \frac{-\hat{S}}{\tau_p} \left(\frac{a_4}{\delta_p^2 - a_p^2} \right),$$

$$\Delta_{101} = \frac{1}{\tau_f} \left[\frac{1}{\psi_f^2 - a_f^2} + \frac{a_2}{\varphi_f^2 - a_f^2} \right] \Delta_{102} = \frac{-1}{\tau_p} \left(\frac{\delta_p a_5}{\delta_p^2 - a_p^2} \right), \Delta_{103} = \frac{1}{\tau_f} \left(\frac{a_1 \psi_f}{\psi_f^2 - a_f^2} + \frac{a_3 \varphi_f}{\varphi_f^2 - a_f^2} \right)$$

$$\Delta_{104} = \frac{1}{\tau_f} \left[\frac{(\sinh \psi_f + a_1 \cosh \psi_f) \psi_f}{\psi_f^2 - a_f^2} + \frac{(a_2 \sinh \varphi_f + a_3 \cosh \varphi_f) \varphi_f}{\varphi_f^2 - a_f^2} \right],$$

$$\Delta_{105} = \frac{1}{\tau_p} \left[\frac{\delta_p (-a_4 \sinh \delta_p + a_5 \cosh \delta_p)}{\delta_p^2 - a_p^2} \right],$$

$$\Delta_{106} = \hat{S} a_f \sinh a_f \cosh a_p + a_p \sinh a_p \cosh a_f,$$

$$\Delta_{107} = \hat{S} a_f \sinh a_p \sinh a_f + a_p \cosh a_f \cosh a_p,$$

$$\Delta_{108} = \Delta_{104} - (\Delta_{100} + \Delta_{101}) a_f \sinh a_f - (\Delta_{102} + \Delta_{103}) \cosh a_f.$$

4 Thermal Marangoni Number

4.1 Case (i): Adiabatic-Adiabatic Boundary Condition

The fluid-porous structure is horizontally enclosed by the adiabatic boundaries. Using the boundary conditions for temperature (25), the distributions $\theta_f(z_f)$ and $\theta_p(z_p)$ are produced by solving (18) and (21):

$$\theta_f(z_f) = A_1[c_1 \cosh a_f z_f + c_2 \sinh a_f z_f + \Sigma_{f2}(z_f)] \tag{32}$$

$$\theta_p(z_p) = A_1[c_3 \cosh a_p z_p + c_4 \sinh a_p z_p + \Sigma_{p2}(z_p)] \tag{33}$$

where $\Sigma_{f2}(z_f) = A_1[\delta_1 - \delta_2 + \delta_3 - \delta_4]$, $\Sigma_{p2}(z_p) = A_1[\delta_5 - \delta_6]$

$$\delta_1 = \frac{(\alpha_{2f} z_f + \alpha_{1f})}{(\psi_f^2 - a_f^2)} (\cosh \psi_f z_f + a_1 \sinh \psi_f z_f),$$

$$\delta_2 = \frac{2\psi_f \alpha_{2f}}{(\psi_f^2 - a_f^2)^2} (a_1 \cosh \psi_f z_f + \sinh \psi_f z_f),$$

$$\delta_3 = \frac{(\alpha_{2f} z_f + \alpha_{1f})}{(\varphi_f^2 - a_f^2)} (a_2 \cosh \varphi_f z_f + a_3 \sinh \varphi_f z_f),$$

$$\delta_4 = \frac{2\varphi_f \alpha_{2f}}{(\varphi_f^2 - a_f^2)^2} (a_3 \cosh \varphi_f z_f + a_2 \sinh \varphi_f z_f),$$

$$\delta_5 = \frac{(\alpha_{1p} + \alpha_{2p} z_p)}{(\delta_p^2 - a_p^2)} (a_4 \cosh \delta_p z_p + a_5 \sinh \delta_p z_p),$$

$$\delta_6 = \frac{2\alpha_{2p} \delta_p}{(\delta_p^2 - a_p^2)^2} (a_5 \cosh \delta_p z_p + a_4 \sinh \delta_p z_p),$$

$$\alpha_{1f} = R_{If}^* - 1, \alpha_{2f} = -2R_{If}^*, \alpha_{1p} = -(R_{Ip}^* + 1), \alpha_{2p} = -2R_{Ip}^*,$$

$$c_1 = c_3 \hat{T} + \Delta_{10} - \Delta_{11}, c_2 = \frac{1}{a_f} (c_4 a_p + \Delta_{12} - \Delta_{13}), c_3 = \frac{\Delta_{19} \Delta_{14} - \Delta_{16} \Delta_{18}}{\Delta_{15} \Delta_{18} + \Delta_{17} \Delta_{14}},$$

$$c_4 = \frac{\Delta_{16} \Delta_{17} + \Delta_{19} \Delta_{15}}{\Delta_{14} \Delta_{17} + \Delta_{18} \Delta_{15}}, \Delta_9 = -[\delta_7 + \delta_8 + \delta_9 + \delta_{10}],$$

$$\delta_7 = \frac{\psi_f (\alpha_{2f} + \alpha_{1f})}{(\psi_f^2 - a_f^2)} (a_1 \cosh \psi_f + \sinh \psi_f),$$

$$\delta_8 = \left[\frac{\alpha_{2f}}{(\psi_f^2 - a_f^2)} - \frac{2\psi_f^2 \alpha_{2f}}{(\psi_f^2 - a_f^2)^2} \right] (\cosh \psi_f + a_1 \sinh \psi_f),$$

$$\delta_9 = \frac{\varphi_f (\alpha_{2f} + \alpha_{1f})}{(\varphi_f^2 - a_f^2)} (a_3 \cosh \varphi_f + a_2 \sinh \varphi_f),$$

$$\delta_{10} = \left[\frac{\alpha_{2f}}{(\varphi_f^2 - a_f^2)} - \frac{2\varphi_f^2 \alpha_{2f}}{(\varphi_f^2 - a_f^2)^2} \right] (a_2 \cosh \varphi_f + a_3 \sinh \varphi_f),$$

$$\Delta_{10} = \hat{T} \left[\frac{\alpha_{1p} a_4}{(\delta_p^2 - a_p^2)} - \frac{2\alpha_{2p} \delta_p a_5}{(\delta_p^2 - a_p^2)^2} \right],$$

$$\Delta_{11} = \frac{\alpha_{1f}}{(\psi_f^2 - a_f^2)} - \frac{2\psi_f a_1 \alpha_{2f}}{(\psi_f^2 - a_f^2)^2} + \frac{a_2 \alpha_{1f}}{(\varphi_f^2 - a_f^2)} - \frac{2\varphi_f a_3 \alpha_{2f}}{(\varphi_f^2 - a_f^2)^2},$$

$$\Delta_{12} = \left[\frac{\alpha_{2p}}{(\delta_p^2 - a_p^2)} - \frac{2\delta_p^2 \alpha_{2p}}{(\delta_p^2 - a_p^2)^2} \right] a_4 + \frac{a_5 \alpha_{1p}}{(\delta_p^2 - a_p^2)},$$

$$\Delta_{13} = \frac{\alpha_{1f} \psi_f a_1 + \alpha_{2f}}{(\psi_f^2 - a_f^2)} - \frac{2\alpha_{2f} \psi_f^2}{(\psi_f^2 - a_f^2)^2} + \frac{\alpha_{1f} \varphi_f a_3 + \alpha_{2f} a_2}{(\varphi_f^2 - a_f^2)} - \frac{2a_2 \alpha_{2f} \varphi_f^2}{(\varphi_f^2 - a_f^2)^2},$$

$$\Delta_{14} = a_p \cosh a_p, \Delta_{15} = a_p \sinh a_p,$$

$$\begin{aligned} \Delta_{16} &= \left[\frac{-\alpha_{2p}}{(\delta_p^2 - a_p^2)} + \frac{2\delta_p^2 \alpha_{2p}}{(\delta_p^2 - a_p^2)^2} \right] (a_4 \cosh \delta_p - a_5 \sinh \delta_p) - \Delta_{160}, \\ \Delta_{160} &= \frac{\delta_p(\alpha_{1p} - \alpha_{2p})}{(\delta_p^2 - a_p^2)} (a_5 \cosh \delta_p - a_4 \sinh \delta_p), \Delta_{17} = \hat{T} a_f \sinh a_f, \\ \Delta_{18} &= a_p \cosh a_f, \Delta_{19} = \Delta_9 - a_f (\Delta_{10} - \Delta_{11}) \sinh a_f - (\Delta_{12} - \Delta_{13}) \cosh a_f \end{aligned}$$

We get tMn by using the expression (23) as

$$M_{t1} = \frac{-A_1 - M_s a_f^2 \bar{U}}{a_f^2 (c_1 \cosh a_f + c_2 \sinh a_f + \Lambda_2 + \Lambda_3)} \tag{34}$$

where

$$\begin{aligned} A_1 &= \psi_f^2 (\cosh \psi_f + a_1 \sinh \psi_f) + \varphi_f^2 (a_2 \cosh \varphi_f + a_3 \sinh \varphi_f), \\ \bar{U} &= c_{13} \cosh a_f z_f + c_{14} \sinh a_f z_f - \frac{1}{\tau_f} \left[\frac{\cosh \psi_f + a_1 \sinh \psi_f}{\psi_f^2 - a_f^2} + \frac{a_2 \cosh \varphi_f + a_3 \sinh \varphi_f}{\varphi_f^2 - a_f^2} \right], \\ A_2 &= \frac{(\alpha_{2f} + \alpha_{1f})}{(\psi_f^2 - a_f^2)} (\cosh \psi_f + a_1 \sinh \psi_f) - \frac{2\psi_f \alpha_{2f}}{(\psi_f^2 - a_f^2)^2} (a_1 \cosh \psi_f + \sinh \psi_f), \\ A_3 &= \frac{(\alpha_{2f} + \alpha_{1f})}{(\varphi_f^2 - a_f^2)} (a_2 \cosh \varphi_f + a_3 \sinh \varphi_f) - \frac{2\varphi_f \alpha_{2f}}{(\varphi_f^2 - a_f^2)^2} (a_3 \cosh \varphi_f + a_2 \sinh \varphi_f) \end{aligned}$$

4.2 Case (ii): Adiabatic-Isothermal Boundary Condition

The lower porous boundary of the combined layer is adiabatic and the upper fluid boundary of the composite layer is isothermal. Using the temperature boundary conditions (26), the distributions $\theta_f(z_f)$ and $\theta_p(z_p)$ are produced by solving (18) and (21):

$$\theta_f(z_f) = A_1 [c_5 \cosh a_f z_f + c_6 \sinh a_f z_f + \Sigma_{f3}(z_f)] \tag{35}$$

$$\theta_p(z_p) = A_1 [c_7 \cosh a_p z_p + c_8 \sinh a_p z_p + \Sigma_{p3}(z_p)] \tag{36}$$

where $\Sigma_{f3}(z_f) = A_1 [\delta_{11} - \delta_{12} + \delta_{13} - \delta_{14}]$, $\Sigma_{p3}(z_p) = A_1 [\delta_{15} - \delta_{16}]$,

$$\begin{aligned} \delta_{11} &= \frac{(\alpha_{4f} z_f + \alpha_{3f})}{(\psi_f^2 - a_f^2)} (\cosh \psi_f z_f + a_1 \sinh \psi_f z_f), \\ \delta_{12} &= \frac{2\psi_f \alpha_{4f}}{(\psi_f^2 - a_f^2)^2} (a_1 \cosh \psi_f z_f + \sinh \psi_f z_f), \\ \delta_{13} &= \frac{(\alpha_{4f} z_f + \alpha_{3f})}{(\varphi_f^2 - a_f^2)} (a_2 \cosh \varphi_f z_f + a_3 \sinh \varphi_f z_f), \\ \delta_{14} &= \frac{2\varphi_f \alpha_{4f}}{(\varphi_f^2 - a_f^2)^2} (a_3 \cosh \varphi_f z_f + a_2 \sinh \varphi_f z_f), \\ \delta_{15} &= \frac{(\alpha_{3p} + \alpha_{4p} z_p)}{(\delta_p^2 - a_p^2)} (a_4 \cosh \delta_p z_p + a_5 \sinh \delta_p z_p), \\ \delta_{16} &= \frac{2\alpha_{4p} \delta_p}{(\delta_p^2 - a_p^2)^2} (a_5 \cosh \delta_p z_p + a_4 \sinh \delta_p z_p), \\ \alpha_{3f} &= R_{If}^* - 1, \alpha_{4f} = -2R_{If}^*, \alpha_{3p} = -(R_{Ip}^* + 1), \alpha_{4p} = -2R_{Ip}^*, \end{aligned}$$

$$\begin{aligned}
 c_5 &= c_7 \hat{T} + \Delta_{21} - \Delta_{22}, c_6 = \frac{1}{a_f} (c_8 a_p + \Delta_{23} - \Delta_{24}), c_7 = \frac{\Delta_{30} \Delta_{25} - \Delta_{27} \Delta_{29}}{\Delta_{28} \Delta_{25} + \Delta_{26} \Delta_{29}}, \\
 c_8 &= \frac{\Delta_{30} \Delta_{26} + \Delta_{27} \Delta_{28}}{\Delta_{29} \Delta_{26} + \Delta_{25} \Delta_{28}}, \Delta_{20} = -[\delta_{17} + \delta_{18} + \delta_{19} + \delta_{20}], \\
 \delta_{17} &= \frac{\psi_f (\alpha_{4f} + \alpha_{3f})}{(\psi_f^2 - a_f^2)} (a_1 \cosh \psi_f + \sinh \psi_f), \\
 \delta_{18} &= \left[\frac{\alpha_{4f}}{(\psi_f^2 - a_f^2)} - \frac{2\psi_f^2 \alpha_{4f}}{(\psi_f^2 - a_f^2)^2} \right] (\cosh \psi_f + a_1 \sinh \psi_f), \\
 \delta_{19} &= \frac{\varphi_f (\alpha_{4f} + \alpha_{3f})}{(\varphi_f^2 - a_f^2)} (a_3 \cosh \varphi_f + a_2 \sinh \varphi_f), \\
 \delta_{20} &= \left[\frac{\alpha_{4f}}{(\varphi_f^2 - a_f^2)} - \frac{2\varphi_f^2 \alpha_{4f}}{(\varphi_f^2 - a_f^2)^2} \right] (a_2 \cosh \varphi_f + a_3 \sinh \varphi_f), \\
 \Delta_{21} &= \hat{T} \left[\frac{\alpha_{3p} a_4}{(\delta_p^2 - a_p^2)} - \frac{2\alpha_{4p} \delta_p a_5}{(\delta_p^2 - a_p^2)^2} \right], \\
 \Delta_{22} &= \frac{\alpha_{3f}}{(\psi_f^2 - a_f^2)} - \frac{2\psi_f a_1 \alpha_{4f}}{(\psi_f^2 - a_f^2)^2} + \frac{a_2 \alpha_{3f}}{(\varphi_f^2 - a_f^2)} - \frac{2\varphi_f a_3 \alpha_{4f}}{(\varphi_f^2 - a_f^2)^2}, \\
 \Delta_{23} &= \left[\frac{\alpha_{4p}}{(\delta_p^2 - a_p^2)} - \frac{2\delta_p^2 \alpha_{4p}}{(\delta_p^2 - a_p^2)^2} \right] a_4 + \frac{a_5 \alpha_{3p}}{(\delta_p^2 - a_p^2)}, \\
 \Delta_{24} &= \frac{\alpha_{3f} \psi_f a_1 + \alpha_{4f}}{(\psi_f^2 - a_f^2)} - \frac{2\alpha_{4f} \psi_f^2}{(\psi_f^2 - a_f^2)^2} + \frac{\alpha_{3f} \varphi_f a_3 + \alpha_{4f} a_2}{(\varphi_f^2 - a_f^2)} - \frac{2a_2 \alpha_{4f} \varphi_f^2}{(\varphi_f^2 - a_f^2)^2}, \\
 \Delta_{25} &= \cosh a_p, \Delta_{26} = \sinh a_p, \\
 \Delta_{27} &= -\frac{\alpha_{3p} - \alpha_{4p}}{(\delta_p^2 - a_p^2)} (a_4 \cosh \delta_p - a_5 \sinh \delta_p) + \frac{2\delta_p \alpha_{4p}}{(\delta_p^2 - a_p^2)^2} (a_5 \cosh \delta_p - a_4 \sinh \delta_p), \\
 \Delta_{28} &= a_f \hat{T} \sinh a_f, \Delta_{29} = a_p \cosh a_f, \\
 \Delta_{30} &= \Delta_{20} - a_f (\Delta_{21} - \Delta_{22}) \sinh a_f - (\Delta_{23} - \Delta_{24}) \cosh a_f.
 \end{aligned}$$

We get tMn from (23) as

$$M_{t2} = \frac{-\Lambda_1 - M_s a_f^2 \hat{U}}{a_f^2 (c_5 \cosh a_f + c_6 \sinh a_f + \Lambda_4 + \Lambda_5)} \tag{37}$$

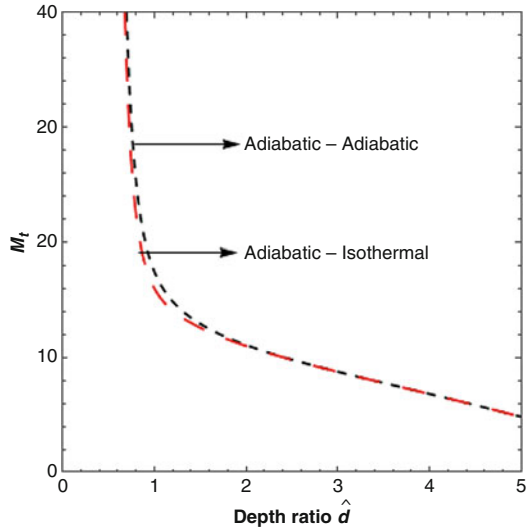
where $\Lambda_4 = \frac{(\alpha_{4f} + \alpha_{3f})}{(\psi_f^2 - a_f^2)} (\cosh \psi_f + a_1 \sinh \psi_f) - \frac{2\psi_f \alpha_{4f}}{(\psi_f^2 - a_f^2)^2} (a_1 \cosh \psi_f + \sinh \psi_f)$,

$$\Lambda_5 = \frac{(\alpha_{4f} + \alpha_{3f})}{(\varphi_f^2 - a_f^2)} (a_2 \cosh \varphi_f + a_3 \sinh \varphi_f) - \frac{2\varphi_f \alpha_{4f}}{(\varphi_f^2 - a_f^2)^2} (a_3 \cosh \varphi_f + a_2 \sinh \varphi_f).$$

5 Results and Discussion

The tMns for two cases of thermal boundary conditions M_{t1} and M_{t2} are obtained as expressions of the depth ratio \hat{d} , the porous parameter β , the thermal ratio \hat{T} , the solutal ratio \hat{S} , sMn M_s and the Chandrasekhar number Q_f , the horizontal wave numbers a_f and a_p , the diffusivity ratio τ_f and τ_p , and R_{If}^* and R_{Ip}^* the modified internal Rayleigh numbers for region 1 and region 2. The thermal boundary conditions taken are adiabatic-adiabatic and that the combined layer is horizontally enclosed by the adiabatic boundaries and adiabatic-isothermal, the lower porous

Fig. 2 Comparison of tMn for case (i) adiabatic-adiabatic and case (ii) adiabatic-isothermal



boundary of the composite system is adiabatic, and the upper fluid boundary of the composite system is isothermal. These tMns M_t are drawn versus the depth ratio \hat{d} using Mathematica software. The other parameters are $a_f = 0.5$, $Q_f = 10$, $\beta = 1.0$, $\hat{\mu} = 2$, $\hat{S} = \hat{T} = 1$, $\tau_f = \tau_p = 0.25$, $M_s = 10$, $R_{ff}^* = 1$ and $R_{fp}^* = 1$, the effects of the various parameters are described in detail and represented in the graphs below.

Figure 2 represents the comparison of M_{t1} and M_{t2} , where M_t is the dependent variable and \hat{d} , the depth ratio, is the independent variable. The tMn decreases up to some value of the depth ratio, and later it increases as the value of the depth ratio also increases. This behavior is qualitatively the same for both types of thermal boundary combination (TBC). It is interesting to note that for larger values of depth ratios, the Marangoni numbers coincide and no change in them for $\hat{d} \geq 2$, i.e., for porous layer dominant (in depth) systems which is physically impressive as the TBC at the boundary of the porous layer is changed. But for the smaller depth ratio values, the thermal Marangoni number for case (i) is smaller than that for case (ii), indicating that the system with case (i) TBC is more stable.

For both situations of TBCs, the effects of the Chandrasekhar number Q_f on double-diffusive Marangoni convection (DDMC) (DDMC) are shown in Fig. 3. The values of Q_f that were used were 1, 10, and 100. The curves are diverging, showing that Q_f is more prominent at higher depth ratios, i.e., for the porous layer dominant composite system (PDCS). Because an increase in the value of Q_f raises the tMns for a certain depth ratio, the DDC can be advanced by lowering the values of Q_f , and the system can be destabilized. This parameter's effect is analogous to that of TBCs.

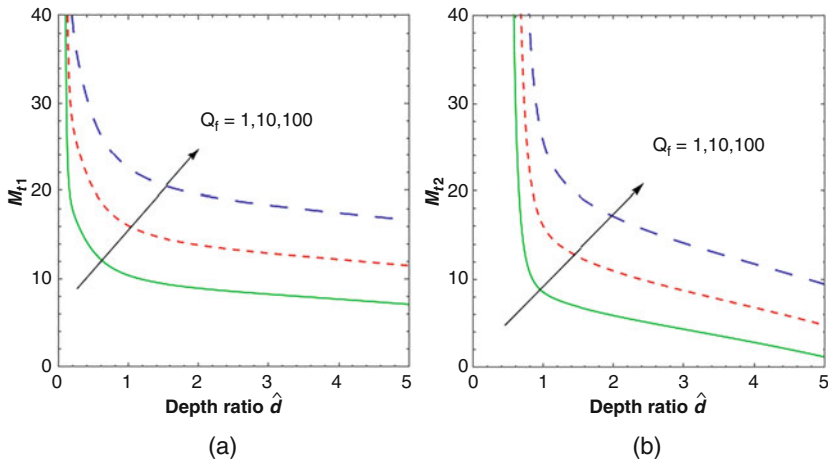


Fig. 3 Variations of $Q_f = 1, 10, 100$ on tMn when $a_f = 0.5, \beta = 1.0, \hat{\mu} = 2, \hat{S} = \hat{T} = 1, \tau_f = \tau_p = 0.25, M_s = 10, R_{If}^* = 1$ and $R_{Ip}^* = 1$

The effect of a modified internal Rayleigh number R_{If}^* on the tMn is shown in Fig. 4 for both the TBCs $R_{If}^* = -1, 0$ and 1 . For larger depth ratio values, i.e., for porous layer dominant composite system (PDCS), the curves diverge, reflecting the importance of the modified internal Rayleigh number. The tMn increases when the value of R_{If}^* is increased, that is, from sink to source, for a certain depth ratio. As a result, the DDMC in the presence of a magnetic field can be delayed by raising the value of R_{If}^* . As a result, the heat absorption stabilizes the system. For TBCs, the effect of this parameter is comparable.

The effect of a modified internal Rayleigh number for porous layer R_{Ip}^* on the tMn is shown in Fig. 5 for $R_{Ip}^* = -1, 0$ and 1 . The Marangoni number grows as the amount of R_{Ip}^* is increased from sink to source; hence, the DDMC in the presence of a magnetic field can be delayed by raising the value of R_{Ip}^* . As a result, the heat absorption stabilizes the system. This parameter has the same effect in both scenarios of TBCs. Also, as shown in the diagram, this parameter is effective for some modest depth ratios, that is, for PDCS in both scenarios of TBCs.

The effect of solute Marangoni number M_s on the Marangoni number is similar for both the cases of TBCs, which is exhibited in Fig. 6 for $M_s = 5, 10$ and 50 . On increasing the values of M_s , the tMn for DDMC in the presence of magnetic field increases; hence, the DDMC can be delayed by increasing the values of M_s . The diverging curves reveal that the effect of sMn is intensive for larger values of depth ratios, that is, for PDCS. The effect of this parameter is comparable to the cases of TBCs.

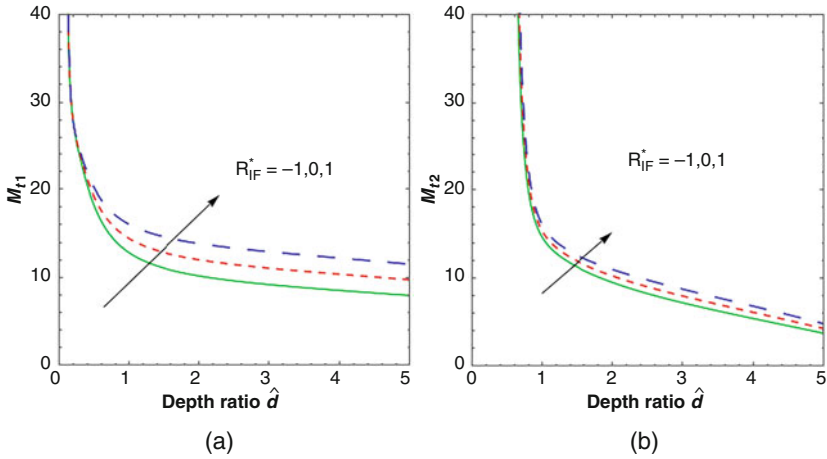


Fig. 4 Variations of $R_{IF}^* = -1, 0, 1$ on tMn when $a_f = 0.5, Q_f = 10, \beta = 1.0, \hat{\mu} = 2, \hat{S} = \hat{T} = 1, \tau_f = \tau_p = 0.25, M_s = 10$ and $R_{Ip}^* = 1$

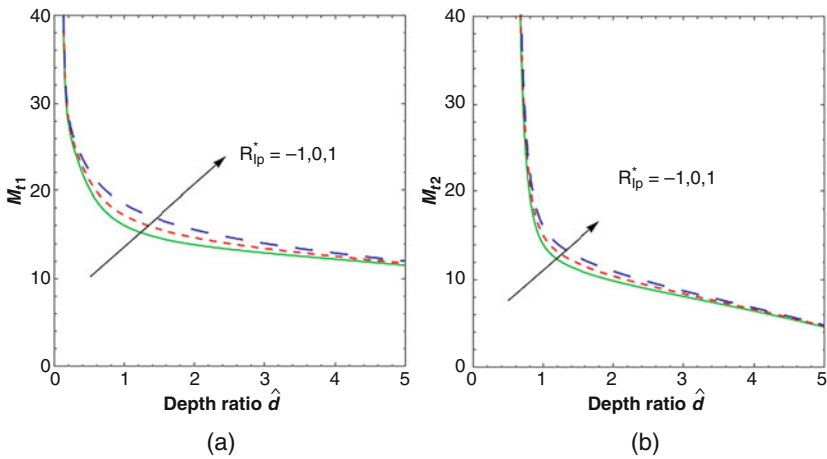


Fig. 5 Variations of $R_{Ip}^* = -1, 0, 1$ for porous region on tMn when $a_f = 0.5, Q_f = 10, \beta = 1.0, \hat{\mu} = 2, \hat{S} = \hat{T} = 1, \tau_f = \tau_p = 0.25, M_s = 10$ and $R_{If}^* = 1$

6 Conclusion

In the current study, the impact of a heat source and magnetic field on onset convection is thoroughly investigated for two different boundary configurations. Because of this, the composite layer system is stable and can be used in adiabatic-adiabatic thermal boundary conditions, where convection needs to be regulated. The following are the key findings from the current study:

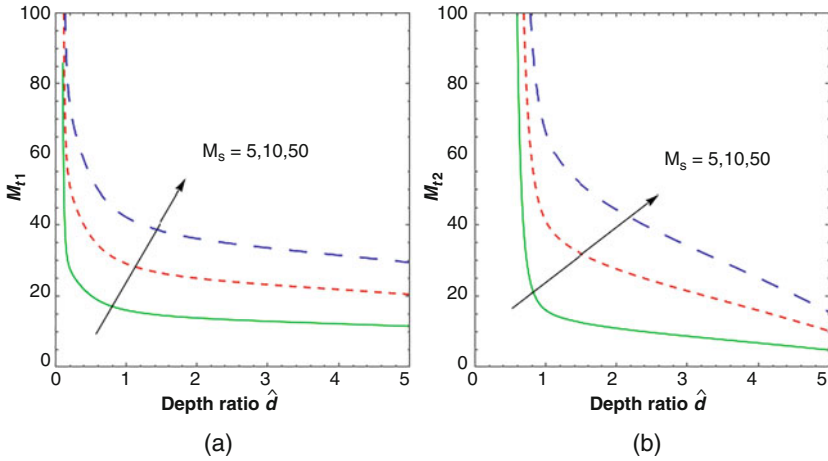


Fig. 6 Variations of $M_s = 5, 10, 50$ on tMn when $a_f = 2.5, Q_f = 10, \beta = 1.0, \hat{\mu} = 2, \hat{S} = \hat{T} = 1, \tau_f = \tau_p = 0.25, R_{If}^* = 1$ and $R_{Ip}^* = 1$

- (i) When compared to the case (ii) thermal boundary condition, the tMn for the case (i) thermal boundary condition is large. As a result, in the case of case (i), the fluid-porous system is stable and can be used in circumstances where convection must be controlled.
- (ii) All the physical parameters are effective for the larger values for depth ratios that are for the PDCS.
- (iii) In the present study, by increasing the values of the Chandrasekhar number Q_f , the modified internal Rayleigh numbers R_{If}^*, R_{Ip}^* , and the solute Marangoni number M_s in the presence of magnetic field, the thermal Marangoni numbers, i.e., to stabilize the system, so the onset of DDMC is delayed.
- (iv) The DDMC in the combined system can be controlled by selecting the proper values for the physical parameters. Results are in good accordance with earlier work.

References

1. Sumithra, R., Manjunatha, N.: Analytical study of surface tension driven magneto convection in a composite layer bounded by adiabatic boundaries. *Int. J. Eng. Innov. Technol.* **1**(6), 249–257 (2012)
2. Sankar, M., Park, Y., Lopez, J.M., Younghae D.: Double-diffusive convection from a discrete heat and solute source in a vertical porous annulus. *Transp. Porous Med.* **91**, 753–775 (2012)
3. Jagadeesha, R.D., Prasanna, B.M.R., Sankar, M.: Double diffusive convection in an inclined parallelogrammic porous enclosure. *Proc. Eng.* **127**, 1346–1353 (2015)
4. Pushpa, B.V., Sankar, M., Makinde, O.D.: Optimization of thermosolutal convection in vertical porous annulus with a circular baffle, *Thermal Sci. Eng. Progress* **20**, 100735 (2020)

5. Moolya, S., Satheesh, A.: Role of magnetic field and cavity inclination on double diffusive mixed convection in rectangular enclosed domain. *Int. Commun. Heat Mass Transfer* **118**, 104814 (2020)
6. Shivakumara, I.S., Raghunatha, K.R., Pallavi, G.: Intricacies of coupled molecular diffusion on double diffusive viscoelastic porous convection. *Results Appl. Math.* **7**, 100124 (2020)
7. Sumithra, R., Arul Selvamary, T.: Single component Darcy-Benard surface tension driven convection of couple stress fluid in a composite layer. *Malaya J. Matematik* **9**(1), 797–804 (2021)
8. Qiang, X., Siddique, I., Sadiq, K., Ali Shah, N.: Double diffusive MHD convective flows of a viscous fluid under influence of the inclined magnetic field, source/sink and chemical reaction. *Alexandria Eng. J.* **59**(6), 4171–4181 (2021)
9. Tanveer, A., Hayat, T., Alsaedi, A.: Numerical simulation for peristalsis of Sisko nanofluid in curved channel with double diffusive convection. *Ain Shams Eng. J.* **12**(3), 3195–3207 (2021)
10. Hussain, S., Jamal, M., Pekmen Geridonmez, B.: Impact of power law fluid and magnetic field on double diffusive mixed convection in staggered porous cavity considering Dufour and Soret effects. *Int. Commun. Heat Mass Transfer* **121**, 105075 (2021)
11. Meften, G.A.: Conditional and unconditional stability for double diffusive convection when the viscosity has a maximum. *Appl. Math. Comput.* **392**, 125694 (2021)
12. Manjunatha, N., Sumithra, R., Vanishree, R.K.: Influence of constant heat source/sink on non-Darcian-Bnard double diffusive Marangoni convection in a composite layer system. *JAMI: J. Appl. Math. Inform.* **40**(1–2), 99–115 (2022)
13. Manjunatha, N., Sumithra, R.: Effects of heat source/sink on Darcian-Bnard-Magneto-Marangoni convection in a composite layer subjected to non uniform temperature gradients. *TWMS J. Appl. Eng. Math.* **12**(3), 669–684 (2022)
14. Shiva kumara, I.S., Suma, S.P., Krishna, B.: Onset of surface tension driven convection in superposed layers of fluid and saturated porous medium. *Arch. Mech.* **58**(2), 71–92 (2006)